Photosynth Res (2008) 95:197–209
DOI 10.1007/s11120-007-9248-z

REGULAR PAPER

Calculation of pigment transition energies in the FMO protein

From simplicity to complexity and back

J. Adolphs · F. Müh · M. E. Madjet · T. Renger

Received: 6 September 2007 / Accepted: 7 September 2007 / Published online: 5 October 2007

Abstract The Fenna–Matthews–Olson (FMO) protein of green sulfur bacteria represents an important model protein for the study of elementary pigment–protein couplings. We have previously used a simple approach [Adolphs and Renger (2006) Biophys J 91:2778–2797] to study the shift in local transition energies (site energies) of the FMO protein of *Prosthecochloris aestuarii* by charged amino acid residues, assuming a standard protonation pattern of the titratable groups. Recently, we have found strong evidence that besides the charged amino acids also the neutral charge density of the protein is important, by applying a combined quantum chemical/electrostatic approach [Müh et al. (2007) Proc Natl Acad Sci USA, in press]. Here, we extract the essential parts from this sophisticated method to obtain a relatively simple method again. It is shown that the main contribution to the site energy shifts is due to charge density coupling (CDC) between the pigments and their pigment, protein and water surroundings and that polarization effects for qualitative considerations can be approximated by screening the Coulomb coupling by an effective dielectric constant.

Keywords Pigment–protein complex · Excitonic coupling · *Prosthecochloris aestuarii* · FMO protein · Site energies · Genetic algorithm

Abbreviations

BChl	Bacteriochlorophyll
CD	Circular dichroism
CDC	Charge density coupling
FMO	Fenna–Matthews–Olson
LD	Linear dichroism
OD	Absorption
PBQC	Poisson–Boltzmann quantum chemistry
PCD	Point charge-dipole
PPC	Pigment-protein complex
RMSD	Root mean square deviation
TrEsp	Transition charge from electrostatic potential

J. Adolphs · F. Müh · M. E.-A. Madjet · T. Renger (✉)
Institut für Chemie und Biochemie, Freie Universität Berlin, Takustrasse 6, Berlin 14195, Germany
e-mail: rth@chemie.fu-berlin.de

Introduction

The pioneering work of biochemists and crystallographers has resulted in high resolution crystal structure data of membrane proteins of astonishing size containing some 10,000s of atoms. Among the largest proteins are those of photosystem I (Jordan et al. 2001) and photosystem II (Ferreira et al. 2004; Loll et al. 2005). These structures open the way for an understanding of the molecular mechanisms of complex reaction schemes like light-harvesting and primary charge separation in photosynthesis. A challenging question that should eventually be answered with these structures is how proteins succeed in functionalizing the same type of cofactor in different ways. Whereas chlorophylls act as light harvesting pigments in the antennae, they perform charge transfer in the reaction center. Clearly, the inter-pigment distances are important, but also the tuning of the optical and electrochemical properties of the pigments by their protein environments. The underlying molecular mechanisms are far from being understood, even for small proteins.

For the latter, there is a chance to obtain the relevant information about the local optical properties (site energies) of cofactors by a fit of optical spectra. These fits provide a critical test for any method that uses a direct calculation

based on the structural data. An important system in this respect is the Fenna–Matthews–Olson (FMO) protein (Blankenship et al. 1995; Olson 2004) which acts as a mediator of excitation energy between the outer antenna system, i.e., the chlorosomes (Egawa et al. 2007), and the reaction center complex (Rémigy et al. 2002). Since the first high resolution crystal structure of the FMO protein appeared more than 30 years ago (Fenna and Matthews 1975), there have been numerous of theoretical approaches trying to explain the low-temperature optical spectra.

In these approaches, the structural data have been used to calculate excitonic couplings between the seven bacteriochlorophyll *a* pigments (BChls) that are bound per FMO monomer and the site energies were treated as fit parameters. Nevertheless, it has been an unsolved problem for more than 20 years to find a satisfying description of the different linear optical spectra and a common set of site energies.

A large part of the puzzle was solved by Aartsma and coworkers (Louwe et al. 1997; Wendling et al. 2002) who used a smaller effective dipole strengths of the BChls in the calculation of excitonic couplings than assumed previously. The smaller excitonic couplings allowed for a simultaneous description of absorption and linear and circular dichroism. We have recently checked (Adolphs and Renger 2006) that the values for the optimal site energies do not change qualitatively, if a more sophisticated theory of optical spectra (Renger and Marcus 2002a) is used that contains vibrational sidebands, life-time broadening and resonance energy transfer narrowing, which were neglected in the original approach (Louwe et al. 1997).

In addition, we presented (Adolphs and Renger 2006) a quantitative explanation of the low effective dipole strength. In this approach, a Poisson equation is solved for the electrostatic potential of transition charges originating from the transition monopole approximation of the $S_0 \rightarrow S_1$ transition of BChl*a* (Chang 1977). The monopoles are positioned in vacuum cavities in the dielectric volume of the protein, where the cavity shapes are determined by van-der-Waals radii of the atoms of the BChl cofactors and the protein volume by the radii of protein atoms.

Recently, we have developed a new method (TrEsp, Madjet et al. 2006) to obtain transition charges from a fit of the electrostatic potential of the ab initio transition density. The coupling from these transition charges was shown to be identical with the one that is obtained in the transition density cube method (Krueger et al. 1998). Here, we will use the TrEsp transition charges and simplify the description of the dielectric environment by including the solvent and assigning the same dielectric constant to the protein and the solvent.

The drawback of a fitting procedure for the site energies is that it is impossible to relate the obtained optimal values to structural details of the pigment–protein complex (PPC). A first attempt of a direct calculation of site energies from structural data was reported by Gudowska-Nowak et al. (1990). Quantum chemical calculations of BChl transition energies were performed taking into account the different conformations of the macrocycles of the BChls, including the acetyl group rotation, and also all charged amino acids in the vicinity of the BChls. However, the reported site energies do not describe the optical spectra, most likely because important long-range electrostatic interactions were neglected in this purely quantum chemical approach.

We have recently used a very simple electrostatic method (Adolphs and Renger 2006) to include all charged amino acids of the protein, assuming a standard protonation pattern. The site energy shifts were obtained from the difference in Coulomb couplings between the charge densities of the charged amino acid residues and the ground and excited state charge densities of the BChls. The former were described by point charges and the latter by the difference permanent dipole moment between ground and excited state. We will therefore term this approach point charge-dipole (PCD) method. A qualitative description of experimental data was obtained, after performing a partial fit of the site energies of those two BChls that are not ligated by His but by Leu (BChl 5) and water (BChl 2). The major drawback of this approach is a too simple description of interactions between BChls and their close environment as is evident from the difference potential between the charge density of the excited and the ground state of BChl*a* (Madjet et al. 2006) in Fig. 1. This potential is clearly different from that of a dipole, and therefore, e.g., hydrogen bond effects to the 13^1-keto and 3-acetyl group are incorrectly described in the PCD approach. The difference potential indicates how a partial charge of the protein varies the transition energy of the BChls. For example, if a positive charge is located in the negative difference potential (shown in red) a stronger stabilization of the excited state and therefore a red shift of the transition energy results.

To take into account both, the short- and the long-range interactions in an appropriate way, we proposed a new calculation method (Müh et al. 2007), combining quantum chemistry with electrostatics in atomic detail. The charge density of both the protein and the pigments was described by atomic partial charges. Moreover, polarization effects of the dielectric of the protein and the solvent were considered as well as a realistic protonation pattern by solving a Poisson–Boltzmann equation and using a Monte Carlo approach to sample the possible protonation states of the titratable residues. We will call this approach the Poisson–Boltzmann quantum chemistry (PBQC) method throughout this article. For the first time, it became possible to reach quantitative agreement between experimental spectra and calculations that essentially contain no free parameters. On this basis, the importance of different parts of the protein could be analyzed.

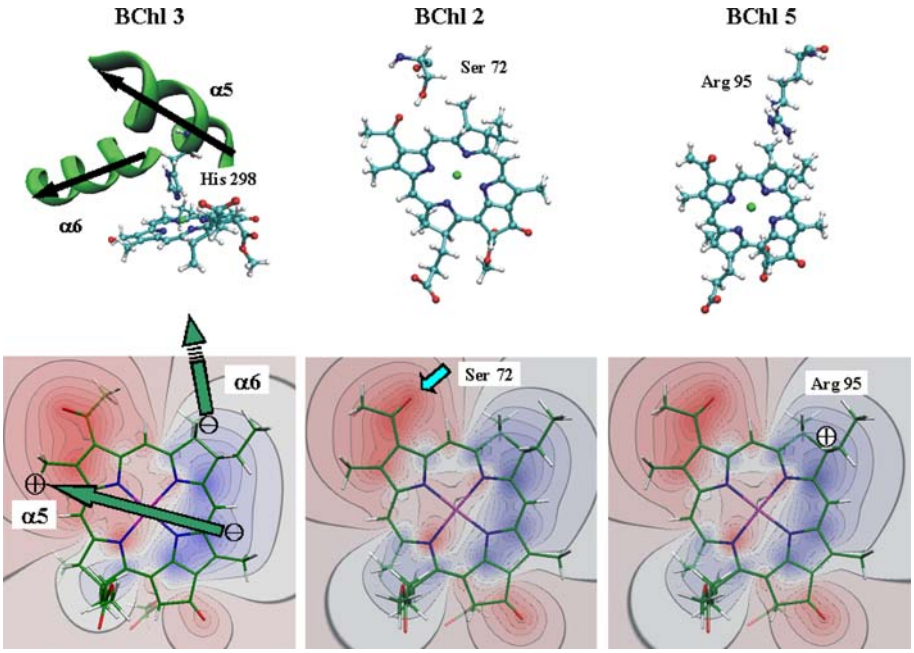

Fig. 1 Dominant influence of local protein environments on optical transition energies of BChls 3, 2, and 5. The upper part contains structural elements (α-helices, hydrogen bond donors, charged amino acid residues) and the lower part places the charge distribution of these elements relative to the difference in electrostatic potential $\Delta\phi(r) = \phi_{11}(r) - \phi_{00}(r)$ between excited state S_1 and ground state S_0 of BChl*a* (Madjet et al. 2006), shown as a contour plot in the plane of the pigment. *Blue:* Positive potential values. *Red:* Negative potential values

Rather unexpectedly, the electric field of the backbone of two α-helices was identified to determine the energy sink at BChl 3 (Müh et al. 2007). Besides this effect, charged amino acids, hydrogen bonds between the keto and acetyl groups of BChls and their protein environment, and other charge density couplings (CDC) contribute to the shifts. Polarization effects and the different conformations of the BChls were found to be least important.

The latter finding provided the inspiration for the present article, where we want to study whether it is possible to simplify the PBQC approach by just taking into account the Coulomb coupling between the charge densities of the ground and excited states of the BChls and those of the protein. In this approach that we term CDC method, any polarization effects are approximated by screening the Coulomb coupling by an effective dielectric constant ε_{eff}. Furthermore, a standard protonation pattern is assumed for the titratable residues.

The article is organized in the following way: A brief summary of the theory of optical spectra and three previous approaches to determine site energies is given. The present CDC approach is discussed next. Afterwards results on the optical spectra of the FMO protein of *P. aestuarii* are presented and the various approaches are compared. The different parts of the pigment–protein interaction that give rise to the site energy shifts are analyzed in detail. Finally, the article is summarized and concluded.

Theory of optical spectra

In the following, a brief overview of the theory of optical spectra is given. For a more detailed discussion we refer to Renger and Marcus (2002a) and Adolphs and Renger (2006).

Hamiltonian

The theory is based on a standard Hamiltonian H_{ppc} for the pigment–protein complex, that describes the pigments as coupled two-level systems interacting with inter- and intramolecular vibrational degrees of freedom. The Hamiltonian H_{ppc} of the PPC consists of three parts:

$$H_{\text{ppc}} = H_{\text{ex}} + H_{\text{ex-vib}} + H_{\text{vib}}. \quad (1)$$

The exciton Hamiltonian H_{ex} contains the site energies E_m of the pigments, defined as the optical transition energies at the equilibrium position of nuclei in the electronic ground state, and the excitonic couplings V_{mn}. The exciton vibrational Hamiltonian $H_{\text{ex-vib}}$ describes the modulation of site energies by the vibrations, that is assumed to be linearly dependent on the nuclear coordinates with the dimensionless coupling constants g_ξ. The key quantity in the expressions for optical spectra and exciton relaxation is the spectral density

$$J(\omega) = \sum_\xi g_\xi^2 \delta(\omega - \omega_\xi) \quad (2)$$

where the g_ξ are assumed to be site-independent, i.e., the same local modulation of site energies by the vibrational dynamics for all BChls is assumed. The spectral density is related to the Huang–Rhys factor S by $\int_0^\infty J(\omega)\, d\omega = S$. The vibrations are described by the Hamiltonian H_{vib} of harmonic oscillators.

For the calculations of optical spectra, $H_{\rm ppc}$ is expressed in terms of delocalized exciton states $|M\rangle$, which are linear combinations of the local excited states $|m\rangle$, $|M\rangle = \sum_m c_m^{(M)}|m\rangle$, where $|c_m^{(M)}|^2$ describes the probability that the mth pigment is excited when the PPC is in the Mth exciton state. The exciton coefficients $c_m^{(M)}$ and energies $\mathcal{E}_M$ are obtained from the solution of the eigenvalue problem

$$H_{\rm ex}|M\rangle = \mathcal{E}_M|M\rangle. \tag{3}$$

The exciton–vibrational Hamiltonian $H_{\rm ex-vib}$ contains diagonal ($M = N$) as well as off-diagonal ($M \neq$ N) elements, which give rise to vibrational sidebands and life-time broadening of optical lines, respectively.

Linear optical spectra

The linear absorption $\alpha(\omega)$ is obtained from the Fourier–Laplace transform of the dipole–dipole correlation function as explained in detail in Renger and Marcus (2002a),

$$\alpha(\omega) \propto \left\langle \sum_M |\mathbf{d}_M|^2 D_M(\omega) \right\rangle_{\rm dis}, \tag{4}$$

where the transition dipole moments $\mathbf{d}_M = \sum_m c_m^{(M)}\mathbf{d}_m$ of the delocalized exciton states are linear combinations of the local transition dipole moments $\mathbf{d}_m$. $D_M(\omega)$ is the lineshape function and $\langle\,\rangle_{\rm dis}$ denotes an average over static disorder in site energies. A Gaussian distribution function of width (fwhm) $\Delta_{\rm dis}$[1] is assumed for these energies, and the disorder average is performed by a Monte Carlo method.

The local transition dipole moments $\mathbf{d}_m$ are assumed to be oriented along the N_B–N_D axis of the BChls. Alternatively the influence of the conformations of the BChls on this orientation is investigated by (i) performing a quantum chemical calculation of the transition density for each BChl separately and constraining the torsional angle of the acetyl group to its value in the crystal structure, (ii) determining TrEsp transition charges $q_I^{(m)}(1,0)$ (Madjet et al. 2006) and placing them on the atom positions $\mathbf{R}_I^{(m)}$ of BChl m of the crystal structure. The transition dipole moment then is obtained as $\mathbf{d}_m = \sum_I q_I^{(m)}(1,0)\mathbf{R}_I^{(m)}$.

In the calculation of circular dichroism (CD), the dipole strength $|\mathbf{d}_M|^2$ in Eq. 4 is replaced by the rotational strength r_M and in the case of linear dichroism (LD) by $|\mathbf{d}_M|^2(1 - 3\cos^2\theta_M)$, where θ_M is the angle between the symmetry axis of the trimer and the exciton transition dipole moment $\mathbf{d}_M$.

The lineshape function $D_M(\omega)$, obtained using a non-Markovian partial ordering prescription (POP) theory (Renger and Marcus 2002a), is given as

$$D_M(\omega) = \frac{1}{2\pi}\int_{-\infty}^{\infty} {\rm d}t\, {\rm e}^{{\rm i}(\omega-\tilde{\omega}_M)t}{\rm e}^{G_M(t)-G_M(0)}{\rm e}^{-|t|/\tau_M}. \tag{5}$$

The vibrational sidebands are described by the time-dependent function $G_M(t)$ and the lifetime broadening by the dephasing time τ_M. $G_M(t)$ contains the spectral density $J(\omega)$, the exciton coefficients $c_m^{(M)}$, a correlation radius $R_{\rm c}$ of protein vibrations[2] and the mean number $n(\omega)$ of vibrational quanta with energy $\hbar\omega$, that are excited at a given temperature T (Bose–Einstein distribution function). The dephasing time τ_M in Eq. 5 is determined by the Redfield rate constants of exciton relaxation (Renger and Marcus 2002a; Adolphs and Renger 2006). The $\tilde{\omega}_M$ in Eq. 5 is shifted from the purely excitonic transition frequency ω_M by the exciton–vibrational coupling. The shift term contains the local reorganization energy and the pigment's optical gap correlation function (Renger and Marcus 2002a). The spectral density $J(\omega)$ is expressed as

$$J(\omega) = SJ_0(\omega). \tag{6}$$

For the normalized function $J_0(\omega)$, we assume that it has the same form as the spectral density, that was extracted recently (Renger and Marcus 2002a) from 1.6 K fluorescence line narrowing spectra of the B777 complex:

$$J_0(\omega) = \frac{1}{s_1+s_2}\sum_{i=1,2}\frac{s_i}{7!2\omega_i^4}\omega^3{\rm e}^{-(\omega/\omega_i)^{1/2}} \tag{7}$$

with the extracted parameters $s_1 = 0.8$, $s_2 = 0.5$, $\hbar\omega_1 = 0.069$ meV and $\hbar\omega_2 = 0.24$ meV. The Huang–Rhys factor S of the pigment–protein coupling in Eq. 6 was estimated (Adolphs and Renger 2006) from the temperature dependence of the absorption spectrum (Freiberg et al. 1997; Wendling et al. 2000) of the FMO complex of *P. aestuarii* to be approximately 0.5.

Excitonic couplings in a dielectric environment

The excitonic couplings are obtained from the Coulomb couplings between the transition densities of the BChls. To take into account the influence of the dielectric, we introduced the following method (Adophs and Renger 2006).

[1] We use different widths for the seven pigments. Pigments 1, 3, 4: fwhm = 60 cm^{-1}; Pigment 2: fwhm = 100 cm^{-1}; Pigments 5–7: fwhm = 120 cm^{-1}. This empirical assignment is based on the assumption that those BChls, which according to the crystal structure have more water molecules bound in their vicinity, should have a larger disorder because of the structural heterogeneity of the water molecules.

[2] A value of $R_{\rm c} = 5$ Å is used, that was determined from transient spectra of photosystem II reaction centers in Renger and Marcus (2002b). The stationary spectra calculated here do not depend critically on this value.

A dielectric volume of the protein is created from overlapping spheres of its atoms with atomic radii taken from the CHARMM22 force field (MacKerell et al. 1998). The transition density of BChl m, is described by atomic transition charges $q_I^{(m)}(1,0)$ that are located in the respective cavities in the FMO protein, $\rho_m(\mathbf{r}) = \sum_I q_I^{(m)}(1,0)\delta(\mathbf{r} - \mathbf{R}_I^{(m)})$. An optical dielectric constant of $\varepsilon = 2$ is assumed for the protein and $\varepsilon = 1$ (i.e. vacuum) for the BChl cavities. The transition charges are rescaled such as to result in the correct magnitude of the vacuum transition dipole moment of 6.1 D as determined in an empty cavity analysis by Knox and Spring (2003) from absorption data of BChl*a* in different solvents. The Poisson equation

$$\nabla \cdot [\varepsilon(\mathbf{r})\nabla\phi_m(\mathbf{r})] = -4\pi \sum_I q_I^{(m)}\delta(\mathbf{r} - \mathbf{R}_I^{(m)}) \tag{8}$$

is solved for each BChl numerically by a finite difference method using the program MEAD (Bashford and Karplus 1990). The value of $\varepsilon(\mathbf{r})$ equals 2 if $\mathbf{r}$ points to a position in the protein and 1 in the case of BChl. From the resulting electrostatic potential $\phi_m(\mathbf{r})$ of the transition density of BChl m, the excitonic coupling with BChl n is given as (Adolphs and Renger 2006)

$$V_{mn} = \int \mathrm{d}\mathbf{r}\phi_m(\mathbf{r})\rho_n(\mathbf{r}) = \sum_I \phi_m(\mathbf{R}_I^{(n)})q_I^{(n)}(1,0) \tag{9}$$

The transition charges $q_I^{(m)}(1,0)$ are obtained from a fit of the electrostatic potential of the transition density (TrEsp, Madjet et al. 2006), obtained with time-dependent density functional theory using a 6-31G* basis set and a B3LYP exchange correlation (XC) functional. A geometry optimization is performed, constraining the torsional angle of the 3-acetyl group to its value in the crystal structure (Tronrud et al. 1986) to study the influence of the acetyl group orientation of the BChls on the excitonic coupling. Alternatively, the coupling is calculated with transition charges obtained for fully geometry optimized BChl*a* (Madjet et al. 2006). In this case, all BChls carry the same set of charges $\{q_I\}$. The quantum chemical calculations were performed with the programs Jaguar (5.5) and QChem (Kong et al. 2000) and the fit of the electrostatic potential with the CHELP-BOW program (Sigfridsson and Ryde 1998).

In a simplified version of the method, the polarizability of the solvent is taken into account, using the same optical dielectric constant $\varepsilon = 2$ as for the protein. In this case, there is no need to create a dielectric volume of the protein, and the BChls are modeled as vacuum cavities in the homogeneous dielectric containing the TrEsp charges. The two different types of dielectrics are illustrated in Fig. 2.

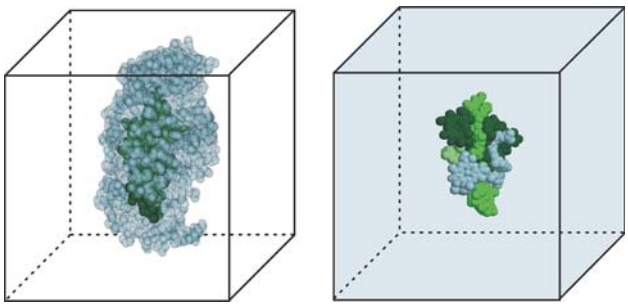

Fig. 2 Dielectric volume considered in the calculations of excitonic couplings. *Left:* The pigments are surrounded by protein with $\varepsilon = 2$, outside of the protein ε equals 1. *Right:* The BChls are surrounded by protein and solvent, both described by $\varepsilon = 2$. In both cases, the BChl shaped cavities have $\varepsilon = 1$ inside

The results obtained by the above methods are compared with a simple point dipole approximation

$$V_{mn} = f \cdot \frac{d_{\mathrm{vac}}^2}{R_{mn}^3}[\mathbf{e}_m \cdot \mathbf{e}_n - 3(\mathbf{e}_m \cdot \mathbf{e}_{mn})(\mathbf{e}_n \cdot \mathbf{e}_{mn})] \tag{10}$$

where $\mathbf{e}_m$ is a unit vector along the transition dipole moment of the mth BChl, the unit vector $\mathbf{e}_{mn}$ is oriented along the line connecting the centers of BChls m and n, and d_{vac}^2 is the dipole strength of the Q_y transition of BChl*a* in vacuum. The factor f describes the enhancement of the dipole strength and the screening of the Coulomb coupling by the dielectric environment in an effective way. It will be investigated, which value of f gives the closest agreement with the values obtained from the electrostatic calculations above. We note that in general f is distance and orientation dependent (Scholes et al. 2007). However, our previous calculations showed that the important nearest neighbor couplings may be approximated by the same f. This finding is supported also by the present calculations.

Calculation of site energies with different methods

In the following, four independent methods to obtain the site energies of the seven BChl*a* molecules of the monomeric subunits of the FMO protein of *P. aestuarii* are described. We first summarize briefly three methods that we have proposed previously (Adolphs and Renger 2006; Müh et al. 2007) and then suggest a new method that is more advanced than the simple electrostatic PCD method (Adolphs and Renger 2006) and simpler than the PBQC approach (Müh et al. 2007) but still captures the important parts of the latter. We start with a summary of a genetic fit algorithm (Adolphs and Renger 2006), which serves as a reference.

Site energies from fit of optical spectra

In this approach, the site energies are obtained indirectly from a fit of optical spectra. A rough description of the optimization process is given in Fig. 3. In the initial step, N sets of site energies are generated (a so-called *population* of N *chromosomes*), one set is provided (start set) and N–1 are randomly created. The corresponding spectra are calculated and the different sets are ranked according to their *fitness value*, which is obtained from the reciprocal of the mean square deviation between the calculated and experimental spectrum. To get better individuals from generation to generation, genetic operations (Kinnebrock 1994; Pohlheim 1999), known as *recombination* and *mutation* (Fig. 3) are performed, taking into account the ranking. In each step, the chromosome with the highest rank is copied to the next cycle (*reproduction*). The fit is iteratively completed. The OD, CD and LD low temperature (4 K) spectra of *P. aestuarii*, measured by Wendling et al. (2002) and their derivatives are used in the fit of site energies by the genetic algorithm. Further details are given in Adolphs and Renger (2006).

Site energies from structural data

In the following, three methods are described that aim at a direct calculation of site energies from the structural data. In these approaches, no absolute site energies but relative site energy shifts are calculated. The site energy E_m for BChl m is given by:

$$E_m = E_0 + \Delta E_m, \tag{11}$$

where the site energy shift ΔE_m is obtained by the methods described below, and the constant E_0 is assumed to be equal for all pigments and will be determined from the overall spectral position in comparison with experiment.

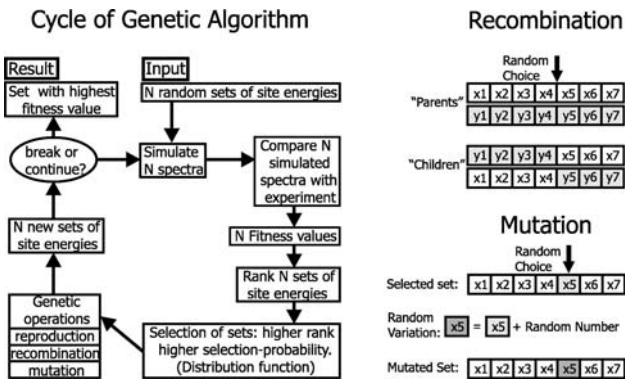

Fig. 3 *Left:* Working scheme of the genetic algorithm used in the fit of optical spectra to obtain the site energies. *Right:* Genetic operations: Recombination (*top*) and mutation (*bottom*)

Point charge-dipole (PCD) method

In the simple electrostatic PCD method, we take into account all amino acid residues that are charged under standard conditions (pH = 7, T = 300 K). They are represented by point charges placed at the respective center of charge, i.e., Arg and Lys are modeled by a positive charge and Asp and Glu by a negative charge (Adolphs and Renger 2006). The electrochromic shift of the site energy E_m of BChl m is then obtained by the Coulomb coupling between these charges and the difference vector $\Delta\mathbf{d}_m$ of permanent dipole moments of the excited and the ground state of BChl m:

$$\Delta E_m = \frac{1}{\varepsilon_{\text{eff}}} \sum_{k=1}^{N} q_k \cdot \frac{\Delta\mathbf{d}_m \cdot \mathbf{r}_{mk}}{r_{mk}^3} \tag{12}$$

where $\mathbf{r}_{mk}$ is the vector connecting the center of the mth pigment with the kth point charge. The effective dielectric constant ε_{eff} in the denominator of Eq. 12 is used to describe the screening and local field effects by the dielectric environment (Steffen et al. 1994).

The difference vector of excited and ground state permanent dipole moments $\Delta\mathbf{d}_m$ is assumed to be of equal magnitude and orientation with respect to the BChl*a* macrocycle for all pigments. From Stark spectra of BChl*a* (Lockhart and Boxer 1987) a value for $|\Delta\mathbf{d}|$ between 1.6 and 2.4 D and an orientation of $\Delta\mathbf{d}$ approximately along the N_B–N_D axis of the BChl can be estimated (Lockhart and Boxer 1987).[3] In the present calculations, we use $|\Delta\mathbf{d}| = 2.0$ D and determine ε_{eff} from the fit of the overall width of the spectrum obtained for the calculated site energies. Further details are given in Adolphs and Renger (2006).

Poisson–Boltzmann quantum chemical (PBQC) method

In this approach, quantum chemistry of BChl*a* in vacuum is combined with electrostatics of the whole protein in atomic detail including polarization effects of the solvent and the protein and an average over the protonation states of the titratable residues (Müh et al. 2007). In short, atomic partial charges of the BChls are obtained by a fit of the electrostatic potential of the ground and excited state charge densities (Madjet et al. 2006). The site energy differences ΔE_m are then obtained by calculating the electrostatic free energy change that occurs when moving the two sets of partial charges from the solvent (with

[3] For BChl*a* in polystyrene (ε = 2.6), a value $|\Delta\mathbf{d}|/f$ of 2–3 was reported (Lockhart and Boxer 1987). Using the empty cavity factor $f = 3\varepsilon/(2\varepsilon + 1)$, then results in $|\Delta\mathbf{d}| = 1.6 - 2.4$.

dielectric constant ε_{solv}) into the specific binding site of BChl *m* in the protein (with dielectric constant $\varepsilon_{protein}$). Further details are given in Müh et al. (2007).

Charge density coupling (CDC) method

In the CDC method, the PBQC approach described above is simplified by (i) assuming a standard protonation pattern and (ii) describing the polarization effects by screening the CDC by an effective dielectric constant ε_{eff}. To evaluate the CDC, two sets of partial charges are needed, $\{\Delta q_I^{(m)}\}$ and $\{q_J^{(bg)}\}$. The $\Delta q_I^{(m)} = q_I^{(m)}(1,1) - q_I^{(m)}(0,0)$ describe the shift in charge density of the PPC when BChl *m* is excited. It is non-zero only on the macrocycle of BChl *m*. The remaining charge density of the PPC is described by the background charges $q_J^{(bg)}$ that include the whole protein, certain water molecules,[4] all BChls $n \neq m$ in the ground state and also the phytyl chain of BChl *m*.

The electrochromic shift of the *m*th pigment is calculated from the Coulomb interaction of the difference of ground and excited state partial charges $\Delta q_I^{(m)}$ of pigment *m* with the background charges $q_J^{(bg)}$

$$\Delta E_m = \frac{1}{\varepsilon_{\text{eff}}} \sum_{I=1}^{N} \sum_{J=1}^{K} \frac{\Delta q_I^{(m)} \cdot q_J^{(\text{bg})}}{|r_I^{(m)} - r_J^{(\text{bg})}|}, \tag{13}$$

where *N* is the number of partial charges of the macrocycle of BChl *m*, *K* is the total number of background partial charges and $|r_I^m - r_J^{(bg)}|$ is the distance between the *I*th difference partial charge of the *m*th pigment and the *J*th partial charge of the background.

The background charges of the protein and the water are taken from the CHARMM22 force field (MacKerell et al. 1998). The partial charges of BChls are obtained from a fit of the ab initio electrostatic potential of the ground and excited state charge densities as described in detail in Madjet et al. (2006). The quantum chemical calculations are either performed on a fully geometry optimized BChl*a* resulting in the same partial charges for all BChls, or after performing a restricted geometry optimization where the torsional angle of the acetyl groups of BChls is kept as in the crystal structure (Tronrud et al. 1986). In the latter case, we also included the direct effect of the acetyl group rotation on the transition energy as obtained from the quantum chemical calculations. The site energy is then obtained as $E_m = E_0 + \Delta E_m + \Delta E_m^{(qc)}$ with ΔE_m in Eq. 13 and adjusting E_0 to describe the spectra. We note that $\Delta E_m^{(qc)}$ is also considered in the PBQC method.

[4] These water molecules are the hydrogen bond donor to the 3-acetyl group of BChl 1, the axial ligand to the Mg atom of BChl 2, and two water molecules bridging the side chains of Asp 234 and Ser 235 via H-bonds.

Results

Excitonic couplings

The excitonic couplings were calculated in vacuum ($\varepsilon = 1$) and in a dielectric ($\varepsilon = 2$) representing the protein (prot) or the protein and the solvent (psol). TrEsp transition monopole charges were used obtained either for fully geometry optimized planar BChl*a* (plan) or taking into account the conformation of the acetyl group (conf). The results of these various calculations are presented in Table 1. As seen from a comparison of columns (1)–(4), there is only a minor influence of the acetyl group conformation on the couplings. The couplings obtained for the *prot* and the *psol* dielectric are also very similar. However, the comparison of these calculations with the vacuum calculations ($\varepsilon = 1$) in columns (5) and (6) shows that there is a reduction of the strongest couplings by about 20% due to the dielectric medium. The excitonic couplings determined by the various TrEsp methods can be well approximated by the point dipole approximation and a factor $f = 0.8$ as seen in the last column of Table 1 and in Fig. 4, where the optical spectra obtained with TrEsp/psol (conf) and PD ($f = 0.8$) are compared to experimental data (Wendling et al. 2002). In the TrEsp calculation, the change in transition dipole orientation ($\mathbf{d}_m$) was taken into account. We find, however, that all transition dipole moments $\mathbf{d}_m$ lie within ± 2° of the N_B–N_D axis of the respective BChl *m*. The site energies of the PBQC approach (Müh et al. 2007) were used in the calculation of the spectra.

Site energy shifts

In Table 2, the site energies obtained by the fit are compared with those of the simple PCD approach (Adolphs and Renger 2006), the sophisticated PBQC method (Müh et al. 2007) and the new CDC approach. The correlation of the directly calculated and the fitted site energies is shown in Fig. 5. There is a significant improvement of the correlation when going from the PCD to the new CDC approach. The correlation of the PBQC site energies with the values from the fit is the highest. The spectra obtained with the various sets of site energies are compared in Fig. 6 with the experimental data (Wendling et al. 2002). The PCD spectra deviate strongly from the experiment, whereas there is a semi-quantitative agreement between the CDC spectra and the experiment. The PBQC calculations describe the experimental OD and LD spectra quantitatively and the CD spectra semi-quantitatively. The CDC and the PBQC method result in nearly the same E_0, whereas the one in the PCD approach is very different.

Table 1 Excitonic couplings for *P. aestuarii* in units of cm^{-1} obtained with different methods explained in detail in the text

BChl	(1) TrEsp plan prot, $\varepsilon = 2$	(2) TrEsp plan psol, $\varepsilon = 2$	(3) TrEsp conf prot, $\varepsilon = 2$	(4) TrEsp conf psol, $\varepsilon = 2$	(5) TrEsp plan vac, $\varepsilon = 1$	(6) TrEsp conf vac, $\varepsilon = 1$	(7) PD, Eq. 10 $f = 0.8$
1–2	**–104**	**–101**	**–101**	**–98**	**–133**	**–130**	**–98**
1–3	5	3	5	3	7	7	5
1–4	–4	–4	–4	–4	–8	–7	–6
1–5	5	4	5	4	9	8	7
1–6	–18	–18	–16	–15	–24	–21	–15
1–7	–8	–8	–7	–7	–12	–11	–14
2–3	**34**	**25**	**33**	**24**	**39**	**38**	**31**
2–4	7	6	7	6	10	10	8
2–5	5	3	6	3	2	3	1
2–6	8	8	8	8	15	14	13
2–7	2	1	2	1	6	6	9
3–4	**–56**	**–52**	**–50**	**–45**	**–81**	**–72**	**–56**
3–5	3	1	–2	0	0	–1	–2
3–6	–8	–6	–8	–6	–11	–11	–10
3–7	6	7	1	2	3	3	3
4–5	**–70**	**–68**	**–71**	**–68**	**–87**	**–88**	**–66**
4–6	–16	–15	–15	–15	–24	–23	–18
4–7	**–58**	**–59**	**–58**	**–59**	**–70**	**–70**	**–58**
5–6	**76**	**77**	**70**	**71**	**97**	**89**	**89**
5–7	7	6	4	3	5	1	–3
6–7	**32**	**27**	**31**	**26**	**40**	**39**	**37**

The strong couplings are highlighted

In accordance with some of the earlier fitting results (Vulto et al. 1998; Wendling et al. 2002), pigment number 3 has the lowest site energy, independent of the method. The overall ranking in site energies obtained here from the fit is exactly identical to that obtained earlier by Wendling et al. (2002).

In Fig. 7, the influence of the acetyl group conformation of BChls on the calculated site energies is investigated by taking into account the conformation of this group in the quantum chemical calculation of partial charges and the transition energy shifts $\Delta E_m^{(qc)}$. Although there are some quantitative differences, the site energies obtained by using the same set of partial charges for all BChls and neglecting $\Delta E_m^{(qc)}$ are very similar. Therefore, all following calculations are performed neglecting the acetyl group conformation in the calculation of BChl partial charges. Here, we use $\varepsilon = 2.5$, as determined from the comparison of calculated CDC spectra and experimental data in Fig. 6.

Influence of certain parts of the PPC

The advantage of a direct structure-based calculation of site energies is, that it is possible to identify the influence of certain parts of the protein. Here, we investigate the influence of the amino acid side chains, the protein backbone, the backbone of the α-helices, the water molecules, the hydrogen bonds and the BChls, using the CDC method. The resulting site energy shifts are summarized in Tables 3–5 and illustrated in Figs. 8 and 9.

As seen in Fig. 8, the site energies of BChls are influenced by all of the contributions considered. Side chains have a large influence on BChls 1, 2, 4 and 5, the protein backbone is important for BChls 3 and 4, H-bonds lead exclusively to red shifts (BChls 1–4, 6) and also the BChl–BChl CDC has some influence (BChls 3, 6, 7). Interestingly, the large red shift of BChl 3 is due to its CDC with the backbone of α-helix 5 and 6 (Müh et al. 2007), as shown in detail in Table 4 and Fig. 9.

In the FMO complex, two types of hydrogen bonds to BChl appear, that differ in the H-bond acceptor group of BChl: H-bonds to the 3-acetyl group and to the 13^1-keto group. Two BChls are without hydrogen bonds (BChls 5[5] and 7), one has a H-bond to a water molecule (BChl 1), and four (BChls 2–4, 6) have up to three H-bonds to amino

[5] The close proximity of one water molecule to the 13^1-keto group of BChl 5 suggests formation of an H-bond there, but in our structural model this water molecule is oriented towards the negatively charged Asp 234, so that no H-bond is formed. Turning the water molecule towards the 13^1-keto group of BChl 5 results in a moderate red shift of $\approx$ 50 cm^{-1}.

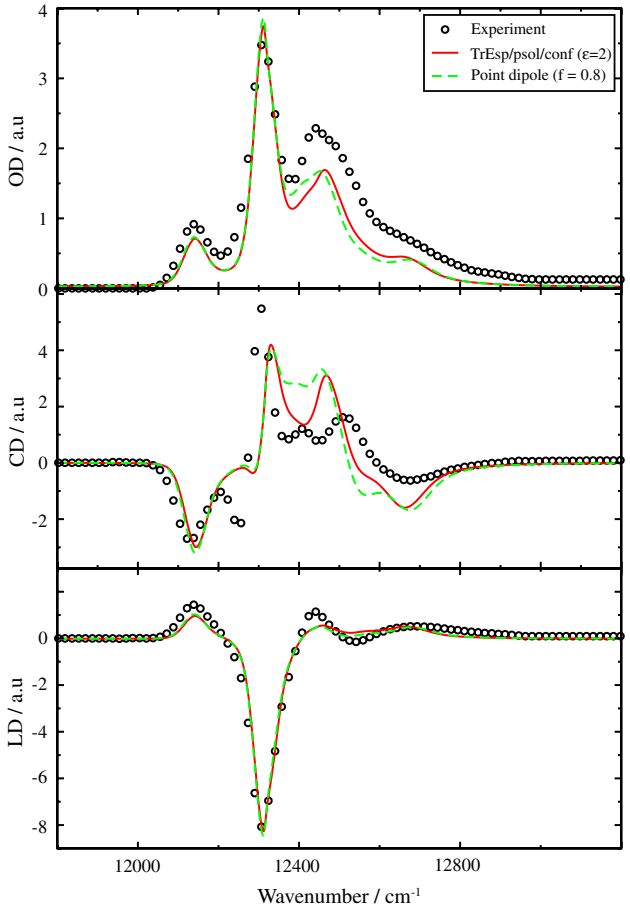

Fig. 4 Comparison of 4 K absorption (OD), circular dichroism (CD) and linear dichroism (LD) experimental data (Wendling et al. 2002) with calculations using site energies from PBQC in Table 2 and different methods for the excitonic couplings: The green dashed curves were obtained for couplings calculated in point dipole approximation with $f = 0.8$, assuming the transition dipoles to be oriented in N_B–N_D direction. The red solid lines were obtained for the TrEsp/prot/solv (conf) couplings including the influence of the BChl conformations on the transition charges and on the orientations of local transition dipole moments $\mathbf{d}_m$

acids (Ala, Arg, Ile, Ser, Trp, Tyr). The detailed contributions of these groups are given in Table 5.

Discussion

Excitonic couplings

The present calculations corroborate our earlier conclusion (Adolphs and Renger 2006) that the excitonic couplings in the FMO protein can be well described by the point-dipole approximation taking into account the influence of the dielectric by an effective dipole strength of $f\,d^2_{vac} = 30\ D^2$. The semi-empirical transition monopole charges of Chang (1977) used previously were replaced here by the ab initio

Table 2 Comparison of site energy shifts obtained directly from the structural data using different methods with values obtained from the fit

BChl	Fit	PCD	PBQC	CDC
1	–90 **4**	305 **7**	–150 **3**	5 **6**
2	–110 **3**	–10 **2**	–60 **5**	–180 **2**
3	–370 **1**	–130 **1**	–365 **1**	–380 **1**
4	–180 **2**	190 **6**	–165 **2**	–85 **4**
5	10 **7**	10 **3**	60 **7**	50 **7**
6	5 **6**	155 **5**	–50 **6**	–70 **5**
7	–85 **5**	90 **4**	–100 **4**	–135 **3**
ε_{eff}	–	1.8	1.8/10.0	2.5
E_0	12560	12320	12560	12540

The values for ε_{eff} and E_0 in PCD and CDC were treated as parameters obtained from comparison with experimental data. The values 1.8/10.0 for the dielectric constant in PBQC refer to the dielectric constants used for the protein and the solvent, respectively. Bold numbers rank the pigments according to their site energies

TrEsp charges (Madjet et al. 2006), taking into account the influence of the acetyl group rotation. In addition, the solvent was included by assigning to it the same ε as to the protein. All of these extensions do not change the effective dipole strength and therefore support our earlier explanation. If at all, there is a slight decrease of the factor f from 0.80 in our earlier calculations to 0.76–0.78 in the present. However, at the present level of theory, we consider such a small change as not significant. The assumption of the same factor f becomes incorrect for the small couplings obtained at large inter-pigment distances

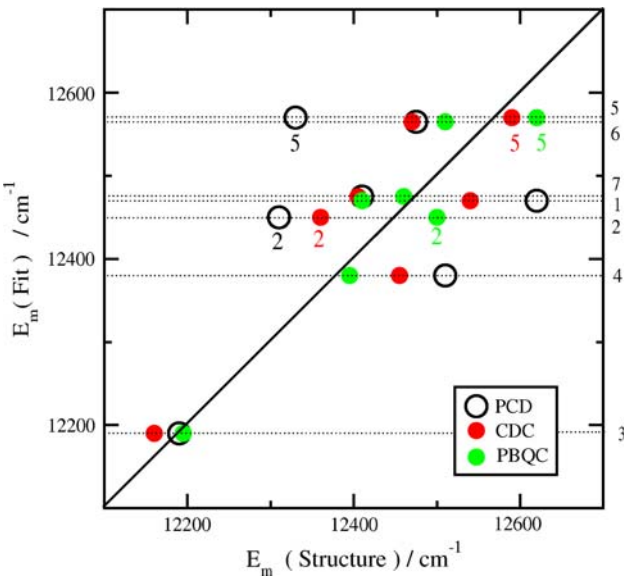

Fig. 5 Correlation of site energies calculated with PCD (black circles), CDC (red circles) and PBQC (green circles) with the site energies from the fit, Table 2. The horizontal lines refer to the pigments (black numbers on the right axis)

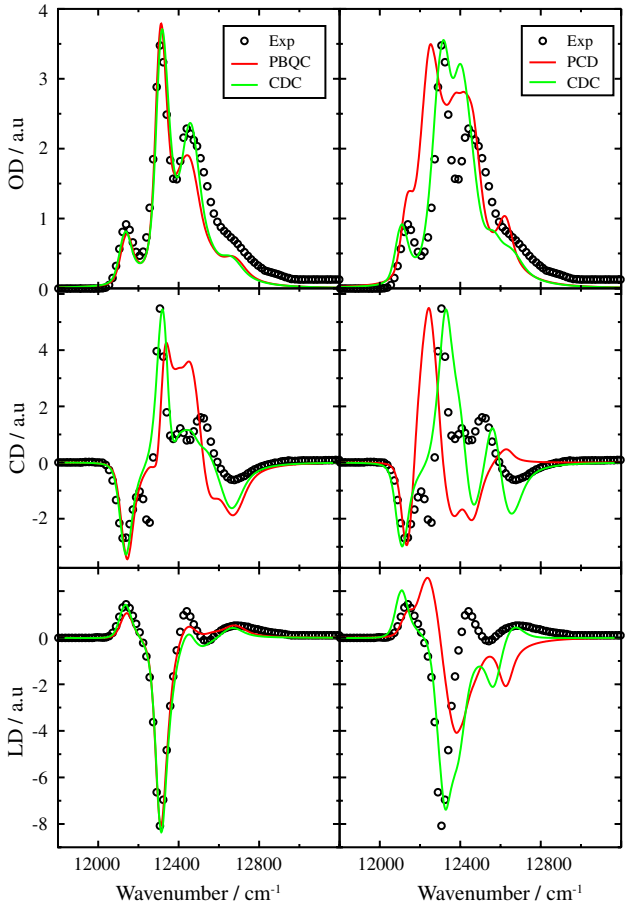

Fig. 6 Comparison of 4 K absorption (OD), circular dichroism (CD) and linear dichroism (LD) experimental data (Wendling et al. 2002) (circles) with calculations, using the site energies obtained with different methods (Table 2) and a point dipole approximation (Eq. 10, $f = 0.8$)

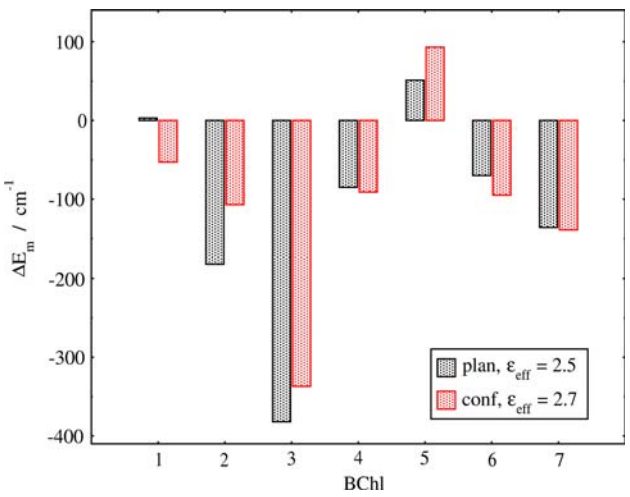

Fig. 7 Site energy shifts ΔE_m/cm^{-1} obtained by using partial charges of fully optimized BChl*a* (plan) or by taking into account the rotation of acetyl groups of the BChls as in the crystal structure (conf)

(Adolphs and Renger 2006). However, the error made for these small couplings does not influence the spectra significantly because of the dominating influence of the nearest neighbour couplings.

Site energies

As seen in Figs. 5 and 6, there is an impressive improvement in accuracy of site energies calculated with the new CDC method compared to our earlier PCD approach. The RMSD between the site energies directly calculated and those obtained from the fit decreases from 245 cm^{-1} in PCD to 65 cm^{-1} in CDC and to 40 cm^{-1} in PBQC. The significant improvement between PCD and CDC demonstrates the importance of the charge density of neutral amino acid residues and of the correct description of the difference potential of BChls, which allows now to describe also hydrogen bonding effects to the 13^1-keto and 3-acetyl groups.

In our earlier PCD calculations, it was necessary to readjust the site energies of BChls 2 and 5 by performing a partial fit. The resulting blue shifts of E_2 and E_5 were ascribed to the different nature of the axial ligands of these BChls, i.e., water and the backbone of Leu, respectively, compared to His (Adolphs and Renger 2006). An inspection of the ligand contributions to the site energy shifts in the CDC approach in Table 3 shows that indeed the strongest blue shifts are obtained for BChl 2 and 5. However, the magnitudes are smaller than predicted by the partial fit, indicating a certain amount of error compensation in our earlier approach.

As with the PBQC approach (Müh et al. 2007), it turns out with the CDC method that the dominating effect on the energy sink at BChl 3 is due to the electric field of the backbone of α-helices 5 and 6. The dipole moments of these α-helices amount to 33 and 37 D, respectively. The large dipole moments of α-helices were suggested to stabilize the structure of helix bundles (Sheridan et al. 1982) and were found important for the tuning of redox potentials in photosynthetic reaction centers (Ishikita et al. 2006). The present and our recent PBQC results (Müh et al. 2007) provide clear evidence that α-helices can tune transition energies of pigments and, in this way, direct the energy flow. The mechanism of this tuning can be understood in the following way. As reported by Sheridan et al. (1982), the electric field of an α-helix can be well approximated by two partial charges of opposite sign and a magnitude of 0.5 *e* placed at the ends of the helix. As seen in Fig. 1 (*left*), the positive partial charge of α-helix 5 is located in the negative difference potential $\Delta\phi$ and the negative partial charge in the positive $\Delta\phi$ of BChl 3. Therefore, a larger stabilization of the excited state and hence a red shift of the site energy results. This red shift is further increased by α-helix

Table 3 Site energy shifts $\Delta E_m/\text{cm}^{-1}$ caused by certain parts of the PPC: side chain groups (SC), ligands (Lig), protein backbone (BB), backbone of α-helices (Hel), explicitly modeled water molecules (Wat), hydrogen bonds (HB) and BChls. The calculations were performed with the CDC approach

BChl	SC	Lig	BB	Hel	Wat	HB	BChl
1	95	15	–5	–25	–95	–85	10
2	–225	65	–20	–25	75	–115	–15
3	15	–35	–320	–225	0	–150	–80
4	130	10	–210	–185	15	–65	–20
5	145	40	–100	–20	30	0	–25
6	–80	0	60	55	25	–115	–75
7	–30	–35	40	115	–50	0	–95

Table 4 Site energy shifts $\Delta E_m/\text{cm}^{-1}$ caused by certain α-helices (only their backbone), obtained with the CDC method

BChl	α-Helix					
	1	2	3	4	5	6
1	5	–35	5	5	0	–5
2	–5	–10	15	10	–20	–15
3	0	–5	–5	5	–145	–75
4	0	0	0	–10	–105	–75
5	–5	–5	0	10	–10	–10
6	0	15	–20	45	25	–10
7	15	20	25	–10	70	–5

Table 5 Site energy shifts $\Delta E_m/\text{cm}^{-1}$caused by hydrogen bond donors, obtained with the CDC method

BChl	H-Bond donor	H-Bond acceptor	$\Delta E_m/\text{cm}^{-1}$
1	H_2O	3-acetyl	–85
2	Ser 72	3-acetyl	–57
	Ile 137 (B)	13^1-keto	–36
	Tyr 138 (B)	13^1-keto	–21
3	Tyr 15	3-acetyl	–103
	Ala 40 (B)	13^1-keto	–48
4	Tyr 345	13^1-keto	–67
5	–	–	–
6	Trp 184	3-acetyl	–40
	Arg 95	13^1-keto	–75
7	–	–	–

In the second column, the hydrogen bond donor is specified, where (B) indicates that the backbone is the H-bond donor. The side chain of Arg 95 is positively charged

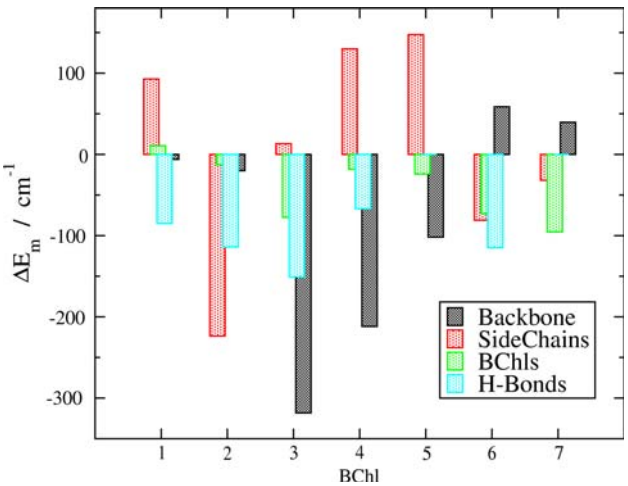

Fig. 8 Site energy shifts $\Delta E_m/\text{cm}^{-1}$ (Table 3) caused by the backbone, side chains, BChls and H-bonds

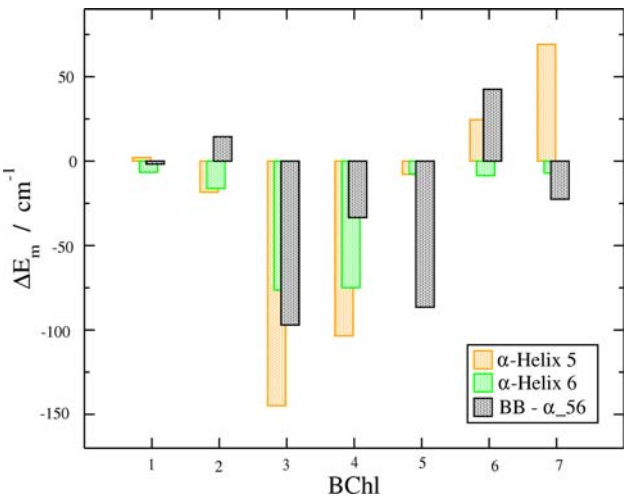

Fig. 9 Site energy shifts $\Delta E_m/\text{cm}^{-1}$ caused by α-helices 5 and 6 and the remaining backbone (Tables 3 and 4)

6 which, however, points away from BChl 3 so that only its negative end contributes significantly.

In qualitative agreement with experimental results on other antenna systems (Fowler et al. 1992), hydrogen bond donors to BChl cause red shifts of the site energies as seen in Fig. 8 and Table 5. The result that hydrogen bonds always lead to red shifts can be understood on the basis of the difference potential in Fig. 1: it is negative around the acetyl and the keto group. A hydrogen bond donor from the

protein will place a partially positively charged hydrogen atom into the negative difference potential, causing thereby a red shift of the transition energy. As an example, the site energy shift of BChl 2 by the hydrogen bond of its 3-acetyl group with Ser 72 is illustrated in Fig. 1 (*center*).

Besides the α-helices and the hydrogen bond donors, the charged amino acid residues influence the site energies. The largest blue shift of a site energy in the present system is caused by the positively charged Arg 95 that is located in the positive $\Delta\phi$ (blue) of BChl 5 (Fig. 1, *right*). We note that this residue is calculated to be protonated in the PBQC approach (Müh et al. 2007), i.e., the standard protonation state assumed in CDC is correct for this group. In general, however, the titratable residues could be in a non-standard state.

Therefore, the best description of experimental data is obtained with the PBQC method, which includes an average over the protonation probabilities and takes into account polarization effects in a more sophisticated way by solving a Poisson–Boltzmann equation. Assuming a standard protonation pattern in the PBQC approach results in a broader spectrum, i.e., the maximal difference between site energies is 495 cm^{-1} compared to 425 cm^{-1} in the non-standard protonation pattern (Müh et al. 2007). This effect is compensated for in the CDC method by using a higher effective dielectric constant, resulting in a maximal site energy difference of 430 cm^{-1}.

We are currently exploiting this result in calculations of the spectral density $J(\omega)$ of the pigment protein coupling by combining CDC with molecular dynamics (MD) simulations. The important advantage of CDC compared to PBQC in this respect is the fast evaluation of the (time-dependent) site energies.

Up to now the $J(\omega)$ has been extracted (Renger and Marcus 2002a) from experiments and the same $J(\omega)$ was assumed for all sites in the calculation of the spectra. With the MD simulations, we plan to compare the spectral densities of all seven pigments, and we will also study the correlation between modulations of different site energies. We aim at a microscopic model for the correlation radius of the exciton–vibrational coupling, that we introduced as an empirical quantity earlier (Renger and May 1998; Renger and Marcus 2002a).

Acknowledgements We would like to acknowledge support by the Deutsche Forschungsgemeinschaft through Emmy-Noether research grant RE 1610 and through the Sonderforschungsbereich 498, TP A7.

References

Adolphs J, Renger T (2006) How proteins trigger excitation energy transfer in the FMO complex of green sulfur bacteria. Biophys J 91:2778–2797

Bashford D, Karplus M (1990) pK_a's of ionizable groups in proteins: atomic detail from a continuum electrostatic model. Biochemistry 29:10,219–10,225

Blankenship RE, Olson JM, Mette M (1995) Antenna complexes from green photosynthetic bacteria. In: Blankenship RE, Madigan MT, Bauer CE (eds) Anoxygenic photosynthetic bacteria. Kluwer Academic Publishers, Dordrecht, pp 399–435

Chang JC (1977) Monopole effects on electronic excitation interaction between large molecules. I. Application to energy transfer in chlorophylls. J Chem Phys 67:3901–3909

Egawa A, Fujiwara T, Mizoguchi T, Kakitani Y, Koyama Y, Akutsu H (2007) Structure of the light-harvesting bacteriochlorophyll *c* assembly in chlorosomes from *Chlorobium limicola* determined by solid-state NMR. Proc Natl Acad Sci USA 104:790–795

Fenna RE, Matthews BW (1975) Chlorophyll arrangement in a bacteriochlorophyll protein from *Chlorobium limicola*. Nature 258:573–577

Ferreira KN, Iverson TM, Maghlaoui K, Barber J, Iwata S (2004) Architecture of the photosynthetic oxygen-evolving center. Science 303:1831–1838

Fowler G, Visschers R, Grief G, van Grondelle R, Hunter C (1992) Genetically modified photosynthetic antenna complexes with blueshifted absorbance bands. Nature 355:848–850

Freiberg A, Lin S, Timpmann K, Blankenship RE (1997) Exciton dynamics in FMO bacteriochlorophyll protein at low temperatures. J Phys Chem B 101:7211–7220

Gudowska-Nowak E, Newton MD, Fajer J (1990) Conformational and environmental effects on bacteriochlorophyll optical spectra: correlations of calculated spectra with structural results. J Phys Chem 94:5795–5801

Ishikita H, Saenger W, Biesiadka J, Loll B, Knapp E (2006) How photosynthetic reaction centers control oxidation power in chlorophyll pairs P680, P700 and P870. Proc Natl Acad Sci USA 103:9855–9860

Jaguar (5.5) Schrödinger, LLC, Portland, OR, 1991–2003

Jordan P, Fromme P, Witt HT, Klukas O, Saenger W, Krauß N (2001) Three-dimensional structure of cyanobacterial photosystem I at 2.5 Å resolution. Nature 411:909–917

Kinnebrock W (1994) Optimierung mit genetischen und selektiven Algorithmen. Oldenbourg

Knox RS, Spring BQ (2003) Dipole strengths in the chlorophylls. Photochem Photobiol 77(5):497–501

Kong J, White CA, Krylov AI, Sherrill CD, Adamson RD, Furlani TR, Lee MS, Lee AM, Gwaltney SR, Adams TR, Ochsenfeld C, Gilbert ATB, Kedziora GS, Rassolov VA, Maurice DR, Nair N, Shao Y, Besley NA, Maslen PE, Dombroski JP, Dachsel H, Zhang WM, Korambath PP, Baker J, Byrd EFC, Van Voorhis T, Oumi M, Hirata S, Hsu CP, Ishikawa N, Florian J, Warshel A, Johnson BG, Gill PMW, Head-Gordon M, Pople JA (2000) Q-Chem 2.0: a high-performance ab initio electronic structure program package. J Comput Chem 21:1532–1548

Krueger BP, Scholes GD, Fleming GR (1998) Calculation of couplings and energy-transfer pathways between the pigments of LH2 by the ab initio transition density cube method. J Phys Chem B 102:5378–5386

Lockhart DJ, Boxer SG (1987) Magnitude and direction of the change in dipole moment associated with excitation of the primary electron donor in *Rhodopseudomonas sphaeroides* reaction centers. Biochemistry 26:664–668

Loll B, Kern J, Saenger W, Zouni A, Biesiadka J (2005) Towards complete cofactor arrangement in the 3.0 Å resolution structure of photosystem II. Nature 438:1040–1044

Louwe RJW, Vrieze J, Hoff AJ, Aartsma TJ (1997) Toward an integral interpretation of the optical steady-state spectra of the FMO-complex of *Prosthecochloris aestuarii*. 2. Exciton simulations. J Phys Chem B 101:11,280–11,287

MacKerell Jr AD, Bashford D, Bellott M, Dunbrack Jr RL, Evanseck JD, Field MJ, Fischer S, Gao J, Guo H, Ha S, Joseph-McCarthy D, Kuchnir L, Kuczera K, Lau FTK, Mattos C, Michnick S, Ngo T, Nguyen DT, Prodhom B, Reiher WE III, Roux B, Schlenkrich M, Smith JC, Stote R, Straub J, Watanabe M, Wiorkiewicz-Kuczera J, Yin D, Karplus M (1998) All-atom empirical potential for molecular modeling and dynamics studies of proteins. J Phys Chem B 102:3586–3616

Madjet ME, Abdurahman A, Renger T (2006) Intermolecular Coulomb couplings from ab initio electrostatic potentials: application to optical transitions of strongly coupled pigments in photosynthetic antennae and reaction centers. J Phys Chem B 110:17,268–17,281

Müh F, Madjet ME, Adolphs J, Abdurahman A, Rabenstein B, Ishikita H, Knapp EW, Renger T (2007) α-helices direct excitation energy flow in the Fenna–Matthews–Olson protein. Proc Natl Acad Sci USA, in press

Olson JM (2004) The FMO protein. Photosynth Res 80:181–187

Pohlheim H (1999) Evolutionäre Algorithmen. Springer, Berlin Heidelberg

Rémigy HW, Hauska G, Müller SA, Tsiotis G (2002) The reaction centre from green sulphur bacteria: progress towards structural elucidation. Photosynth Res 71:91–98

Renger T, Marcus RA (2002a) On the relation of protein dynamics and exciton relaxation in pigment–protein complexes: an estimation of the spectral density and a theory for the calculation of optical spectra. J Chem Phys 116:9997–10,019

Renger T, Marcus RA (2002b) Photophysical properties of PS-2 reaction centers and a discrepancy in exciton relaxation times. J Phys Chem B 106:1809–1819

Renger T, May V (1998) Ultrafast exciton motion in photosynthetic antenna systems: the FMO-complex. J Phys Chem A 102: 4381–4391

Scholes GD, Curutchet C, Mennucci B, Cammi R, Tomasi J (2007) How solvent controls electronic energy transfer and light harvesting. J Phys Chem B 111:6978–6982

Sheridan RP, Levy RM, Salemme F (1982) α-helix dipole model and electrostatic stabilization of 4-α-helical proteins. Proc Natl Acad Sci USA 79:4545–4549

Sigfridsson E, Ryde U (1998) Comparison of methods for deriving atomic charges from the electrostatic potential and moments. J Comp Chem 19:377–395

Steffen M, Lao K, Boxer S (1994) Dielectric asymmetry in the photosynthetic reaction center. Science 264:810–816

Tronrud DE, Schmid MF, Matthews BW (1986) Structure and X-ray amino acid sequence of a bacteriochlorophyll a protein from *Prosthecochloris aestuarii* refined at 1.9 Å resolution. J Mol Biol 188:443–454

Vulto SIE, de Baat MA, Louwe RJW, Permentier HP, Neef T, Miller M, van Amerongen H, Aartsma TJ (1998) Exciton simulations of optical spectra of the FMO complex from the green sulfur bacterium *Chlorobium tepidum* at 6 K. J Phys Chem B 102:9577–9582

Wendling M, Pullerits T, Przyjalgowski MA, Vulto SIE, Aartsma TJ, van Grondelle R, van Amerongen H (2000) Electron–vibrational coupling in the Fenna–Matthews–Olson complex of *Prosthecochloris aestuarii* determined by temperature-dependent absorption and fluorescence line-narrowing measurements. J Phys Chem B 104:5825–5831

Wendling M, Przyjalgowski MA, Gülen D, Vulto SIE, Aartsma TJ, van Grondelle R, van Amerongen H (2002) The quantitative relationship between structure and polarized spectroscopy in the FMO complex of *Prosthecochloris aestuarii*: refining experiments and simulations. Photosynth Res 71:99–123